This paper is dedicated to the late Professor Deane K. Smith as a tribute to his memory and as a mark of respect for the contribution he made to this project.

Outcomes of the International Union of Crystallography Commission on Powder Diffraction Round Robin on Quantitative Phase Analysis: samples 2, 3, 4, synthetic bauxite, natural granodiorite and pharmaceuticals

Nicola V. Y. Scarlett,[a]* Ian C. Madsen,[a] Lachlan M. D. Cranswick,[b] Thaung Lwin,[c] Edward Groleau,[d] Gregory Stephenson,[d] Mark Aylmore[e] and Nicki Agron-Olshina[a]

[a]CSIRO Minerals, Box 312, Clayton South 3169, Victoria, Australia, [b]School of Crystallography, Birkbeck College, Malet Street, Bloomsbury, London WC1E 7HX, UK, [c]CSIRO Mathematical and Information Sciences, Private Bag 10, Clayton South MDC 3169, Australia, [d]Eli Lilly and Company, Lilly Corporate Center, Indianapolis, Indiana 46285, USA, and [e]CSIRO Minerals, PO Box 90, Bentley 6982, Western Australia, Australia. Correspondence e-mail: nicola.scarlett@csiro.au

The International Union of Crystallography (IUCr) Commission on Powder Diffraction (CPD) has sponsored a round robin on the determination of quantitative phase abundance from diffraction data. The aims of the round robin have been detailed by Madsen *et al.* [*J. Appl. Cryst.* (2001), **34**, 409–426]. In summary, they were (i) to document the methods and strategies commonly employed in quantitative phases analysis (QPA), especially those involving powder diffraction, (ii) to assess levels of accuracy, precision and lower limits of detection, (iii) to identify specific problem areas and develop practical solutions, (iv) to formulate recommended procedures for QPA using diffraction data, and (v) to create a standard set of samples for future reference. The first paper (Madsen *et al.*, 2001) covered the results of sample 1 (a simple three-phase mixture of corundum, fluorite and zincite). The remaining samples used in the round robin covered a wide range of analytical complexity, and presented a series of different problems to the analysts. These problems included preferred orientation (sample 2), the analysis of amorphous content (sample 3), microabsorption (sample 4), complex synthetic and natural mineral suites, along with pharmaceutical mixtures with and without an amorphous component. This paper forms the second part of the round-robin study and reports the results of samples 2 (corundum, fluorite, zincite, brucite), 3 (corundum, fluorite, zincite, silica flour) and 4 (corundum, magnetite, zircon), synthetic bauxite, natural granodiorite and the synthetic pharmaceutical mixtures (mannitol, nizatidine, valine, sucrose, starch). The outcomes of this second part of the round robin support the findings of the initial study. The presence of increased analytical problems within these samples has only served to exacerbate the difficulties experienced by many operators with the sample 1 suite. The major difficulties are caused by lack of operator expertise, which becomes more apparent with these more complex samples. Some of these samples also introduced the requirement for skill and judgement in sample preparation techniques. This second part of the round robin concluded that the greatest physical obstacle to accurate QPA for X-ray based methods is the presence of absorption contrast between phases (microabsorption), which may prove to be insurmountable in some circumstances.

1. Introduction

Previous round robin studies in powder diffraction have addressed structural refinement using the method of Rietveld (Hill, 1992; Hill & Cranswick, 1994) and quantification based primarily on the external-standard method (Rafaja &

Valvoda, 1996). In 1996, the Commission on Powder Diffraction (CPD) of the International Union of Crystallography (IUCr) undertook a broader comparison of laboratories and methods in the field of quantitative phase abundance determination from diffraction data. The first sample in the trial
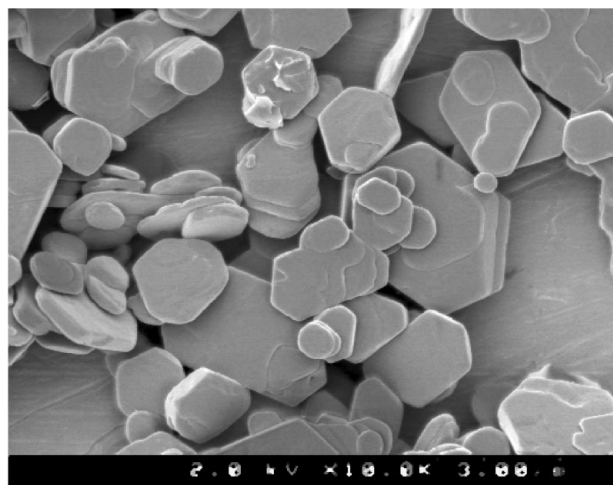
Figure 1
Brucite morphology showing the flat hexagonal plates which lead to preferred orientation along the [00*l*] direction.

(designated sample 1) comprised eight variations of a three-phase mixture which was deemed to present little difficulty to the diffraction analyst. That is, the phases (corundum, fluorite, zincite) were chosen so as to provide minimal microabsorption, preferred orientation, peak broadening and peak overlap. The results of the sample 1 analyses have been presented by Madsen *et al.* (2001). The subsequent samples considered for the round robin were designed specifically to enhance the analytical problems avoided by the sample 1 suite.

Sample 2 is composed of the same materials as the sample 1 suite, but with the addition of brucite [Mg(OH)$_2$]. The brucite chosen has a strongly anisotropic crystal shape with relatively large dimensions in the [*hk*0] plane and small dimensions in the [00*l*] direction (Fig. 1). The flat plate-like morphology induces strong enhancement of the 00*l* reflections as a result of sample packing.

Sample 3 has been included to test the ability of participants to determine the level of amorphous material present in multiphase mixtures. Like sample 2, it has the same basic components as sample 1 (corundum, fluorite, zincite) but with the addition of amorphous silica flour. For those participants analysing CPD data, it was necessary to provide the concentration of at least one component phase (in this case corundum), to act as an internal standard, thus allowing the calculation of the amount of amorphous material in the sample.

Sample 4 presented a microabsorption problem and is composed of corundum, coarse-grained magnetite and zircon. Table 1 shows the mass absorption coefficients (MACs) for each of the phases over a wide range of X-ray wavelengths. It can be clearly seen that there is no wavelength at which the X-ray absorption contrast between the phases will not result in a microabsorption problem. To compound this problem, the material was supplied as a coarse grained powder with the grain size of the phases being 28.0 μm for corundum, 36.2 μm for magnetite and 21.1 μm for zircon. The data supplied by the CPD, collected using Cu $K\alpha_{1,2}$ radiation, was of this unmilled specimen and as such the relative intensities of the phases were strongly affected by microabsorption.

The synthetic bauxite sample emulates a natural bauxite and was included as an example of a complex seven-phase mineral suite. Accordingly, it exhibits many of the problems inherent in such suites, including varying degrees of microabsorption, preferred orientation and peak overlap. A synthetic material was chosen for ease of assessment of results since the 'true' concentration of each phase is known from the weighed amounts.

The natural granodiorite sample was included as an additional example of a complex mineral suite of general interest to the mineralogical community. It also consists of seven easily identified phases, but there remains the possibility for the presence of minor phases not easily detected by diffraction techniques. In this instance, the 'correct' answer is unknown since the granodiorite is a naturally occurring material. In addition, the exact composition of each of the component phases may vary from the nominal values reported in the literature. Phases in this sample are subject to problems such as microabsorption and preferred orientation, and issues such as peak shift, caused by changes in phase composition, further complicate the analysis.

The pharmaceutical samples were included to determine the state of quantitative phase analysis in a less traditional field. Techniques such as powder X-ray diffraction (XRD) are not routinely used in the pharmaceutical sector as they are in

Table 1
X-ray mass absorption coefficients (MAC) for each of the phases used in sample 4 and synthetic bauxite at a wide range of wavelengths.

Phase	Formula	MAC (cm^2 g^{-1})						
		Ti $K\alpha$ (2.750 Å)	Cr $K\alpha$ (2.291 Å)	Fe $K\alpha$ (1.937 Å)	Co $K\alpha$ (1.790 Å)	Cu $K\alpha$ (1.542 Å)	Mo $K\alpha$ (0.711 Å)	Ag $K\alpha$ (0.561 Å)
Corundum	Al$_2$O$_3$	169.8	100.3	61.5	48.8	31.4	3.2	1.6
Magnetite	Fe$_3$O$_4$	153.5	92.1	57.6	46.2	224.6	27.3	14.1
Zircon	ZrSiO$_4$	396.1	241.9	152.9	123.0	81.3	9.4	30.0
Anatase	TiO$_2$	90.2	357.1	230.6	187.1	125.1	14.3	7.3
Boehmite	AlOOH	152.8	90.2	55.3	43.8	28.2	2.8	1.4
Goethite	FeOOH	141.0	84.5	52.7	42.2	196.4	23.8	12.3
Haematite	Fe$_2$O$_3$	150.5	90.3	56.4	45.2	217.5	26.4	13.6
Quartz	SiO$_2$	190.2	113.1	69.7	55.4	35.8	3.6	1.8
Gibbsite	Al(OH)$_3$	130.6	76.9	47.1	37.3	24.0	2.4	1.2
Kaolinite	Al$_2$Si$_2$O$_5$(OH)$_4$	163.5	96.8	59.5	47.2	30.4	3.1	1.5

Table 2
Phase contents of the samples derived from (i) the weighed amounts (where applicable), (ii) the elemental analyses determined by X-ray fluorescence (XRF, where applicable) and (iii) quantitative phase analysis (QPA) using X-ray diffraction methods.

QPA #1 refers to the use of the *SR5* program derived from *LHPM1* of Hill & Howard (1986), while QPA #2 refers to the *KoalaRiet* program described by Coelho *et al.* (1997). QPA #3 refers to the use of the standardless method of Knudsen *et al.* (1981). For XRF, QPA #1, QPA #2 and QPA #3, the values reported represent the means of at least three separate determinations, while the e.s.d.'s are the estimated standard deviations of the means.

	Weighed wt%	XRF wt%	XRF e.s.d.	QPA#1 wt%	QPA#1 e.s.d.	QPA#2 wt%	QPA#2 e.s.d.	QPA#3 wt%	QPA#3 e.s.d.
Sample 2									
Corundum	21.27	20.9	0.8	21.4	0.4	21.4	0.4	21.7	2.1
Fluorite	22.53	24.1	2.9	22.5	0.2	22.5	0.2	20.7	2.0
Zincite	19.94	19.5	0.6	19.9	0.2	19.9	0.2	24.4	2.4
Brucite	36.26	36.1	1.3	36.3	0.7	36.3	0.7	33.2	6.5
Sample 3									
Corundum	30.79	31.1	0.2	30.7	0.0	30.8	0.0	29.8	0.2
Fluorite	20.06	19.9	0.1	20.6	0.1	19.5	0.2	19.6	0.2
Zincite	19.68	19.6	0.1	20.0	0.2	20.0	0.1	21.3	0.1
Amorphous	29.47	27.1	0.1	28.6	0.3	29.7	0.3	29.2	0.2
Sample 4									
Corundum	50.46	50.4	0.2	54.1	2.3	54.5	1.0	–	–
Magnetite	19.64	19.6	0.1	17.0	1.9	16.4	2.6	–	–
Zircon	29.90	29.5	0.1	28.9	1.2	29.1	1.8	–	–
Synthetic bauxite									
Anatase	2.00	–	–	–	–	2.1	0.1	–	–
Boehmite	14.93	–	–	–	–	13.7	0.0	–	–
Goethite	9.98	–	–	–	–	10.5	0.4	–	–
Hematite	10.00	–	–	–	–	9.6	0.3	–	–
Quartz	5.16	–	–	–	–	6.0	0.3	–	–
Gibbsite	54.90	–	–	–	–	54.9	1.2	–	–
Kaolinite	3.02	–	–	–	–	3.2	0.3	–	–
Granodiorite									
Quartz		–	–	29.2	1.5	29.0	2.1	–	–
Feldspar		–	–	19.7	2.1	20.2	3.0	–	–
Albite		–	–	40.4	1.0	40.0	1.4	–	–
Biotite		–	–	7.3	0.6	7.3	0.8	–	–
Clinochlore		–	–	2.3	0.4	2.2	0.6	–	–
Hornblende		–	–	1.1	0.2	1.2	0.3	–	–
Zircon		–	–	0.0	0.0	–	–	–	–

the minerals environment. It is an area that the community might be able to expand into and provide more routine support if the expertise can be developed. The samples supplied contained large particles (leading to poor powder statistics if data were collected on the unmilled specimens) and phases exhibiting a high degree of preferred orientation, which complicated the sample-related issues in data collection.

Table 2 provides a summary of the known proportions for each sample along with values determined by the authors as part of the verification of mixing. These values include (i) the weighed amounts (where applicable), (ii) abundances derived from the elemental analyses determined by X-ray fluorescence (XRF) and (iii) quantitative phase analysis (QPA) by the authors using three different methods of analysis of X-ray diffraction data.

The round robin described here and by Madsen *et al.* (2001) is, as much as anything else, a survey of instrumentation and methods in current usage across a range of laboratories. In the spirit of such a survey, very little was prescribed by the CPD in

the way of detail regarding practices. This means that finer details of participants' data collection and analysis strategies have not always been returned and thus statistical analysis has been limited to the categories which were returned by the majority. Such details of methodology may be addressed in future round robins and cover such information as (i) whether the use of $K\alpha_1$ only, in place of the more conventional $K\alpha_{1,2}$, brings any improvement, (ii) the Rietveld refinement strategy employed, including the choice of preferred-orientation model and details of its implementation [*i.e.* vectors used in the March–Dollase correction method (Dollase, 1986) or the number of terms used in a spherical harmonics series (Von Dreele, 1997; Leventouri, 1997)], and (iii) parameters resulting from refinement, such as R_{wp} and R_{Bragg} values or atomic thermal vibration parameters.

2. Experimental

2.1. Sample preparation

Samples 2 and 3 were prepared in a similar fashion to sample 1 (Madsen *et al.*, 2001), that is by mixing with a hand blender (20000 r.p.m.) under petroleum spirit for approximately 10 min, filtering and drying at 383 K, then coarse sieving to break up the filter cake. Sample 4 was dry mixed by tumbling for approximately 16 h in a large plastic container with 20 small ceramic mixing balls. This procedure was adopted to prevent phase segregation arising from particle size and density differences.

The brucite used in sample 2 is a flame-retardant grade brucite produced at CSIRO Minerals from a purified magnesium chloride liquor *via* an ammonia addition to precipitate the brucite. This purification was followed by hydrothermal treatment (~2 h at ~473 K) to grow the crystals. The approximate particle size of the final material was 2.9 μm as determined by Malvern Mastersizer laser sizing.

Sample 3 contained a proportion of silica flour (Ajax precipitated silica, Batch 53208) with particle size of ~30.4 μm (Malvern Mastersizer). Sample 4 contained the same corundum as used for samples 1, 2 and 3, but also magnetite (natural Malmberget magnetite, particle size ~36.2 μm) and zircon (natural Western Australian zircon, particle size ~21.1 μm). The magnetite was prepared by wet sieving and retaining only the <38 μm fraction. The zircon was prepared by grinding in a large steel mill for 2 min, sieving through a 38 μm sieve, returning the large fraction to the mill for regrinding, then removing the <10 μm fraction *via* a cyclone.

The synthetic bauxite sample was prepared by initially dry mixing the iron oxide mineral components of the mixture (goethite and hematite) separately from the remaining

minerals. The two groups of minerals were tumbled in ceramic mixing vessels containing 2, 5 and 10 mm ceramic mixing balls. The two groups were then combined, divided into two portions and mixed for 2 h under ethanol. They were then recombined and the procedure repeated. At final recombination the sample was left to dry at room temperature. When dry, it was collected in its entirety, coarsely sieved (75 μm) and racked back and forth to break up any lumps formed on drying and to enhance homogeneity.

The granodiorite samples were prepared from a block of Harcourt granodiorite collected near Lancefield in Victoria, Australia.[1] The block, which weighed approximately 5 kg, was broken into pieces of 2–4 cm diameter using a hammer. These pieces were fed through a Sturtevant Jaw Crusher to reduce the particle size to approximately 1.5 mm. Portions of approximately 100 g of crushed material were milled for 1 min in a Siebtechnik Ring Mill to reduce it to the particle size of the samples provided in the round robin. After milling, the granodiorite was mixed thoroughly, then riffled into sub-samples to produce the 3 g and 10 g samples distributed in this study. Additional sample preparation, especially by X-ray users, was at the discretion of the participants.

The composition and details of components of the two pharmaceutical mixtures are given in Table 3. The materials were mixed in a ribbon blender, comprising a helical mixing ribbon, bottom-mounted drive package and clean-sweep bottom blade. They were initially passed through a sieve to break up the large chunks then mixed for approximately 5 min. Vials were then filled to a uniform level.

2.1.1. Verification of mixing. The sample mixtures as supplied were verified using XRF and/or XRD methods. XRD data were collected on random samples from the bulk mixtures and analysed using two separate Rietveld (Rietveld, 1969) programs, *SR5* (Hill & Howard, 1986), and *KoalaRiet* (Coelho *et al.*, 1997), as well as the standardless method of Knudsen (1981). For sample 4 and natural granodiorite, comparisons were made between the relative peak intensities from different XRD data sets to assure uniformity. Where XRF was used, the phase abundances have been calculated from the chemical compositions provided by the analyses.

3. Results

3.1. Summary of participant methodology

From the original sample issue of 128 packages, a total of 49 participants proceeded beyond sample 1 to provide the analyses summarized in this paper (Fig. 2). 40 participants opted to collect their own data and 27 analysed CPD-supplied data, with considerable overlap between these groups. As with sample 1, the greatest number of returns in participant-collected data used XRD techniques. This reflects the prevalence of laboratory-based XRD equipment within the community.

[1] From the same location as the granodiorite sample detailed by Hill *et al.* (1993).

Table 3
Composition of the synthetic pharmaceutical mixtures.

Phase	Description	Pharmaceutical 1 (wt%)	Pharmaceutical 2 (wt%)
Mannitol	Common sugar	45.0	20.0
Sucrose	Common sugar	35.0	15.0
DL-Valine	Amino acid	10.0	20.0
Nizatidine	Active ingredient in the Axid, a medicine for duodenal ulcers and gastric reflux	10.0	15.0
Starch flowable powder	Amorphous polymer produced and stored by plants	0.0	30.0

Samples 2, 3 and 4 collectively provided 61 analyses of CPD-supplied data and 141 analyses of participant-collected data. The synthetic bauxite and granodiorite samples together yielded 26 analyses of CPD-supplied data and 54 analyses of participant-collected data. Disappointingly, the pharmaceutical samples (1 and 2) returned only two analyses of CPD-supplied data and ten of participant-collected data. This indicates a general reluctance within the community to tackle what is perceived as a specialist area with its associated problems.

3.1.1. Instrument type. All data distributed by the CPD were collected using a Philips X'Pert X-ray diffractometer, Cu $K\alpha_{1,2}$, LFF, 40 kV, 40 mA, 1° divergence, 0.3 mm receiving and 1° scatter slits, curved graphite, post-diffraction monochromator, scan range $5-150°$ 2θ for sample 4, synthetic bauxite and granodiorite, and 5–100° 2θ for the pharmaceutical samples, all in steps of 0.02°, with a counting time of 3 s step^{-1}. The CPD-supplied data were collected on the samples as distributed to the participants with the exception of the granodiorite sample which was ground prior to data collection [McCrone micronizing mill (McCrone Research Associates, London), 5 min g^{-1}]. It was up to the participants to decide, when collecting their own data, whether further sample preparation was required or not.
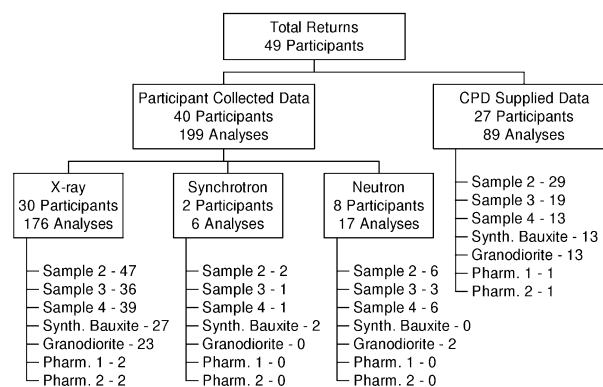

Figure 2
Summary of returns for CPD-supplied and participant-collected data for samples 2, 3, 4, synthetic bauxite, granodiorite and pharmaceuticals. Unless otherwise indicated, the numbers represent the number of analyses in each group.

Fig. 3 gives a breakdown of the wavelengths and diffraction geometries employed for the participant-collected data. By far the greatest number of analyses came from laboratory X-ray users. In the previous study of sample 1, the majority of X-ray data sets were collected using Cu $K\alpha$ radiation. In this current study some 90 analyses have been derived from Co $K\alpha$ data, 75 with Cu $K\alpha$, four using Fe $K\alpha$ and two not specifying the wavelength. Most X-ray data sets were collected using conventional Bragg–Brentano geometry (159), with a few opting for transmission (8) or a fixed angle between the sample surface and the incident beam (6).

The majority of neutron returns (13) used fixed-wavelength instruments (wavelengths ranging from 1.33 to 1.54 Å) with four using time-of-flight geometry (*d*-spacing range collected from 0.47 to 6.3 Å). All neutron returns used capillary geometry. The synchrotron participants all used fixed wavelengths (with individual participants using wavelengths ranging from 0.41 to 1.15 Å) with five data sets collected with capillary geometry and one with a flat plate sample.

3.1.2. Analysis methods. For both participant-collected and CPD-supplied data, by far the most analyses were performed using Rietveld-based methods, with up to ten different Rietveld software packages employed. The next most commonly used analysis technique was the reference intensity ratio (RIR) method with participant-collected data. A few (3) also opted to use this method with CPD data. The remainder used iterative least squares, full-pattern matching or internal-standard methods. A breakdown of analytical methods used is given in Fig. 4.

3.2. Statistical method of results analysis

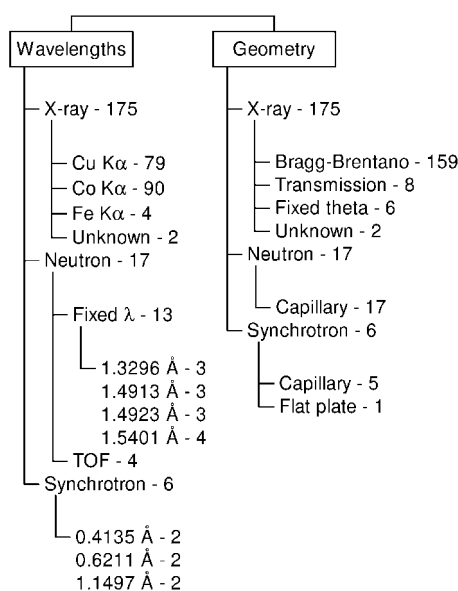A detailed explanation of the statistical methods used for data analysis is provided in the paper detailing sample 1 of this round robin (Madsen *et al.*, 2001). The single numerical assessment of performance for each analysis was derived from the Kullback–Leibler distance (KLD) (Kullback, 1968). The conventional equation for this term has been weighted to allow for the concentration of the phase and is defined as

$$KLD = 0.01 \times wt\%_{True} \times \ln\left(\frac{wt\%_{True}}{wt\%_{Measured}}\right). \quad (1)$$

For an individual sample, an estimate of the Kullback–Leibler distance for all *n* phases can be estimated by summing the KLD values for each phase according to

$$KLD_{sum} = \sum_{i=1}^{n} KLD_i. \quad (2)$$

Where a general estimate of the magnitude of error within an analysis was required, rather than the source of the error, absolute values of the Kullback–Leibler distances (AKLD) have been calculated thus:

$$AKLD_{sum} = \sum_{i=1}^{n} AKLD_i. \quad (3)$$

Accurate analyses are reflected in a low value of AKLD.

To assess the significance of the variation of AKLD within a group, an approximate estimate of the 95% confidence limits can be obtained by first determining the standard deviation (s.d.) of all values of AKLD in the group and calculating the uncertainty according to

$$Uncertainty = \frac{2 \times standard\ deviation\ of\ AKLD}{N^{1/2}}, \quad (4)$$

where *N* is the number of values in the group. This is based upon the assumption that a population of sufficient size will approximate a normal distribution. The smaller the population, the more approximate the estimate.

Figure 3
The wavelengths and instrument geometries for all data collected by participants for samples 2, 3, 4, synthetic bauxite, granodiorite and pharmaceutical samples 1 and 2. The number after each entry represents the number of analyses (including replicates) in each group.
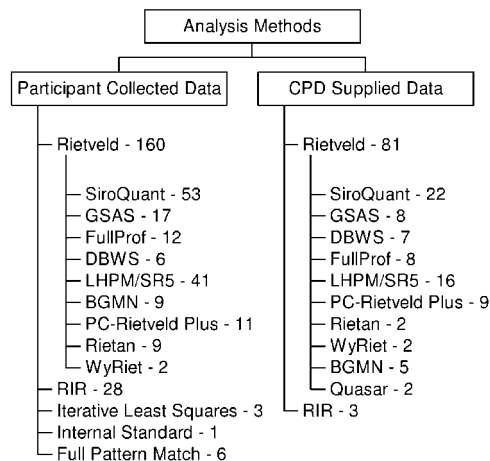
Figure 4
The analytical methods and, for the Rietveld method, the software used for analysis of data (i) collected by participants and (ii) supplied by the CPD for samples 2, 3, 4, synthetic bauxite, granodiorite and pharmaceutical samples 1 and 2. The number after each entry represents the number of analyses (including replicates) in each group.

3.3. Results analysis

The number of returns in each category limits the assessment of results within this study. It is not appropriate to attach much statistical significance to the synchrotron and neutron results, as there are no more than six analyses for any one sample and often fewer (see Fig. 2). In view of this it is only possible to examine problems with individual returns rather than look for trends within a group.

The results are presented for each individual sample to assess the analytical strategies used for each particular problem. The combined AKLDs have also been used to provide an overview of instrumentation and analysis type for all samples in order to compare the performance of the different techniques directly across a wide range of analytical problems. These combined results have been included in an attempt to provide information pertinent to particular laboratory and analytical setups for the range of samples considered here.

Determination of amorphous content in sample 3 was revealed as one of the major analysis problems. In many instances participants had analysed the data solely for the three crystalline phases and normalized them to 100 wt%, omitting to make an appropriate calculation for the amorphous content. This was in spite of its obvious presence in the diffraction pattern (Fig. 5). This will be discussed in greater
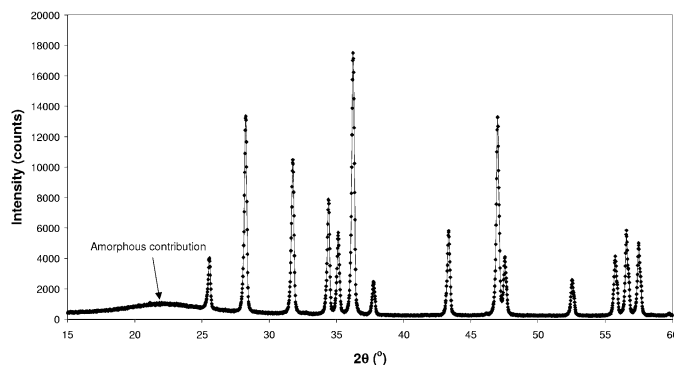

Figure 5
A section of the observed diffraction pattern for sample 3 collected using Cu $K\alpha$ X-rays. Note the presence of the increased pattern background between 15 and 30° 2θ caused by the presence of amorphous material in the sample.

detail in §3.3.3, which deals specifically with sample 3. However, it is mentioned here because it greatly affects the overall performance analysis. Results are therefore presented here which consider the 'as-received' returns as well as results obtained by correction of the sample 3 returns by the authors. This correction has taken the form of normalizing the returned results to the known corundum concentration (30.79 wt%) and determining the amorphous content as the difference

Table 4
Summary of the quantitative phase analyses derived from data (i) supplied by the CPD and (ii) collected by the participants for sample 2.

In addition, the results from participant-collected data have been divided into sub-groups determined by the type of radiation used, namely (i) laboratory X-ray diffraction, (ii) neutron diffraction, and (iii) synchrotron radiation. All values are expressed as wt%. The statistics include all participant determinations including replicates. N represents the total number of measurements included in the statistics for each group. The s.d. value is the standard deviation of the mean, while Min. and Max. represent the minimum and maximum values in each group, respectively. The '50th %' includes only those data with an AKLD value less than or equal to the 50th percentile in the group (*i.e.* CPD-supplied or participant-collected data) and thus represents the most accurate 50% of the returns. Note that for neutron and synchrotron returns, all values reported fell within the 50th percentile of the participant-collected data group.

| Phase | Weighed | CPD-supplied data | | Participant-collected data | | | |
| | | | | X-ray | | Neutron | Synchrotron |
		All data	50th %	All data	50th %	All data	All data
Corundum							
Mean	21.27	21.78	21.51	22.08	21.73	21.76	22.53
s.d.		2.60	0.68	3.28	1.19	0.67	0.54
Min.		12.62	19.80	13.39	19.40	20.60	22.15
Max.		29.00	22.20	39.00	24.01	22.60	22.91
Fluorite							
Mean	22.53	22.11	22.18	22.25	22.59	21.98	22.79
s.d.		2.81	0.70	2.98	1.01	0.43	0.95
Min.		12.22	21.40	11.00	20.00	21.26	22.12
Max.		28.00	23.70	26.20	24.00	22.51	23.46
Zincite							
Mean	19.94	19.58	19.29	18.18	18.95	20.03	19.49
s.d.		5.18	0.51	2.03	0.73	0.94	0.83
Min.		11.08	18.40	9.40	17.90	18.71	18.90
Max.		36.50	20.60	23.00	20.70	21.19	20.07
Brucite							
Mean	36.26	36.53	37.03	36.72	36.72	36.23	35.19
s.d.		7.35	0.79	3.98	1.07	1.07	2.29
Min		18.90	35.70	18.90	35.00	34.38	33.57
Max.		64.07	38.30	43.01	39.30	37.36	36.81
N		29	15	47	20	6	2

Table 5
Summary of the quantitative phase analyses derived from data (i) supplied by the CPD and (ii) collected by the participants for sample 3.

Conventions and definitions are as per Table 4. The 'as received' results are a summary of the values returned by the participants where, in some cases, the amorphous content had not been calculated. An additional section summarizing values where this correction has been made by the authors has been included for completeness. Note that for synchrotron returns, all values reported fell within the 50th percentile of the participant-collected data group.

| Phase | Weighed | CPD-supplied data | | Participant-collected data | | | | |
| | | | | X-ray | | Neutron | | Synchrotron |
		All data	50th %	All data	50th %	All data	50th %	All data
Sample 3 (as received)								
Corundum								
Mean	30.79	34.62	30.63	33.50	31.37	40.06	30.70	32.90
s.d.		6.51	0.36	5.56	0.77	8.18	–	–
Min.		27.84	29.75	30.00	30.79	30.70	30.70	32.90
Max.		46.60	30.80	49.50	33.00	45.85	30.70	32.90
Fluorite								
Mean	20.06	21.78	20.63	20.96	21.09	24.77	18.70	18.90
s.d.		5.81	2.40	5.08	2.44	5.25	–	–
Min.		8.90	18.40	9.00	18.00	18.70	18.70	18.90
Max.		33.10	25.10	33.33	26.10	27.82	18.70	18.90
Zincite								
Mean	19.59	20.83	18.70	19.10	18.22	24.41	18.30	15.50
s.d.		5.04	2.04	4.17	1.42	5.41	–	–
Min.		8.90	14.40	8.90	14.90	18.30	18.30	15.50
Max.		28.39	21.60	29.36	20.80	28.60	18.30	15.50
Amorphous								
Mean	29.42	28.77	29.94	28.88	29.40	10.77	32.30	32.70
s.d.		10.92	3.85	9.27	3.45	18.65	–	–
Min.		0.90	22.50	0.18	3.80	0.00	32.30	32.70
Max.		51.40	35.00	51.20	34.10	32.30	32.30	32.70
N		19	10	36	18	3	1	1
Sample 3 (corrected for amorphous content by authors)								
Corundum								
Mean	30.79	31.71	30.63	32.08	31.40	30.76	30.76	32.90
s.d.		3.74	0.36	3.44	0.78	0.05	0.05	–
Min.		27.84	29.75	30.00	30.79	30.70	30.70	32.90
Max.		44.57	30.80	49.50	33.00	30.79	30.79	32.90
Fluorite								
Mean	20.06	19.93	20.17	20.19	20.42	19.00	19.00	18.90
s.d.		4.51	2.12	4.95	2.06	0.53	0.53	–
Min.		8.90	18.40	9.00	18.00	18.68	18.68	18.90
Max.		27.67	23.98	33.33	24.00	19.60	19.60	18.90
Zincite								
Mean	19.59	19.08	18.50	18.33	17.96	18.72	18.72	15.50
s.d.		3.91	0.83	3.59	1.27	1.30	1.30	–
Min.		8.90	17.50	8.90	14.90	17.68	17.68	15.50
Max.		26.87	19.83	29.36	20.40	20.18	20.18	15.50
Amorphous								
Mean	29.42	29.23	30.61	29.44	30.30	31.52	31.52	32.70
s.d.		9.74	2.12	9.06	3.04	1.84	1.84	–
Min.		0.90	27.55	0.18	25.70	29.42	29.42	32.70
Max.		51.40	33.20	51.20	34.10	32.85	32.85	32.70
N		19	10	36	17	3	3	1

between 100 and the sum of the corrected phase weight percents.

3.3.1. Summary of returned results. Tables 4–9 provide summaries of the quantitative phase analyses derived from CPD-supplied data and participant-collected data for samples 2, 3 and 4, synthetic bauxite, granodiorite and the pharmaceutical samples, respectively. The results from participant-collected data have been subdivided into groups determined by the type of radiation used, namely (i) laboratory X-ray diffraction, (ii) neutron diffraction, and (iii) synchrotron radiation. The statistics for 'all data' include all participant determinations including replicates. The statistics for the '50th %' include only that data with an AKLD value less than or equal to the 50th percentile for that sample. Note that the 50th

Table 6
Summary of the quantitative phase analyses derived from data (i) supplied by the CPD and (ii) collected by the participants for sample 4.

Conventions and definitions are as per Table 4.

| Phase | Weighed | CPD-supplied data | | Participant-collected data | | | | |
| | | | | X-ray | | Neutron | | Synchrotron |
		All data	50th %	All data	50th %	All data	50th %	All data
Corundum								
Mean	50.46	63.60	57.37	57.21	53.26	51.73	51.36	43.19
s.d.		15.56	14.30	7.34	2.00	1.48	1.31	–
Min.		35.00	35.00	41.60	50.20	49.85	49.85	43.19
Max.		80.40	71.91	77.60	56.10	53.58	53.08	43.19
Magnetite								
Mean	19.64	13.52	21.51	18.63	19.47	21.58	20.06	20.90
s.d.		14.80	16.54	5.72	2.53	3.80	0.76	–
Min.		0.60	5.60	0.80	15.30	19.10	19.10	20.90
Max.		46.00	46.00	36.70	24.40	29.21	21.12	20.90
Zircon								
Mean	29.90	22.93	21.21	24.27	27.54	26.71	28.61	35.90
s.d.		9.99	3.41	4.78	2.42	4.70	0.77	–
Min.		16.00	16.10	13.00	23.80	17.22	27.30	35.90
Max.		54.70	25.00	34.00	32.30	29.30	29.30	35.90
N		13	7	39	18	6	5	1

percentile statistics have been omitted where group numbers are insufficient to support such a calculation. Similar omissions have also been made from Table 9 (pharmaceutical samples) because of the low number of returns in this area, making the calculation of such statistics meaningless. Figs. 6, 7 and 8 show individual results for all participants for samples 2, 3 and 4.[2] Despite the large spread in results for CPD-supplied data and participant-collected X-ray data, the mean values for each phase in each sample are in reasonable agreement with the weighed values. The exceptions to this are the results derived from CPD-supplied data for sample 4 and synthetic bauxite. In both these cases extra sample preparation was required to reduce the particle size in sample 4 and to achieve phase liberation in synthetic bauxite. The CPD-supplied X-ray data for the synthetic bauxite was collected on the sample as supplied to the participants. This sample, although fine grained, appeared to have agglomerated in the final mixing process with the effect that the gibbsite particles were probably 'coated' with other phases, causing a suppression of the diffracted gibbsite intensity and a relative enhancement of the peaks of other phases. This selective agglomeration is probably the result of the coexistence of phases of different degrees of density and hardness in the same sample.

3.3.2. Sample 2 – preferred-orientation problem. Fig. 9 shows a summary of the type of preferred-orientation correction applied during data analysis for sample 2. Tables 10 and 11 show the average AKLD values for all returned results partitioned according to preferred-orientation correction method employed for CPD-supplied and participant-collected data, respectively.

There is little difference between the AKLD values for CPD-supplied data and participant-collected data (Tables 10 and 11). In both instances spherical harmonics appears significantly to be the best correction method employed. However, the population of this group is only two, which means such a difference could be purely a reflection of operator expertise rather than the result of the correction method itself. For both CPD-supplied and participant-collected data, the application of any method of correction (whether spherical harmonics or March–Dollase) appears better than the absence of correction. However, the spread of values within the groups in which no correction was applied is so great that the level of uncertainty regarding these figures renders the differences statistically insignificant.

3.3.3. Sample 3 – amorphous-content problem. For sample 3, some participants have neglected to calculate the amorphous content after completing the analysis of the crystalline components (Table 5). To overcome the bias which would be introduced into the statistical analysis, the authors have performed the post-refinement calculation of amorphous content on their behalf. This allows the separation of the real problems in analytical methodology from simple operator error. Some results from both the CPD-supplied data and participant-collected X-ray data show very low, but non-zero, minima for amorphous content. The results providing these low minima cannot be corrected by the authors as they represent a problem that is more severe than mere omission of calculation of amorphous content. Both results were provided by the same participant and are the result of the inclusion of crystalline quartz as a model for the amorphous silica phase in the Rietveld refinement process. It would appear that quartz is not appropriate to model the increase in background intensity (Fig. 5) and in this instance the participant has left the half-

---

[2] Figs. 6, 7 and 8 are available in the online version of this article and from the IUCr electronic archives (Reference: HW0096). Services for accessing these data are described at the back of the journal.
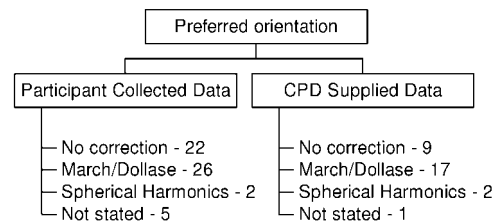
Table 7
Summary of the quantitative phase analyses derived from data (i) supplied by the CPD and (ii) collected by the participants for synthetic bauxite.

Conventions and definitions are as per Table 4.

Phase	Weighed	CPD-supplied data		Participant-collected data		
				X-ray		Synchrotron
		All data	50th %	All data	50th %	All data
Anatase						
Mean	2.00	3.00	2.72	2.37	2.29	1.67
s.d.		0.43	0.38	0.68	0.66	2.06
Min.		2.20	2.20	1.00	1.10	0.21
Max.		3.50	3.20	3.60	3.30	3.12
Boehmite						
Mean	14.93	20.34	20.81	13.80	14.14	13.67
s.d.		2.19	1.23	3.02	1.60	4.65
Min.		16.60	19.43	6.20	11.70	10.38
Max.		23.9	22.7	18.62	17.91	16.95
Goethite						
Mean	9.98	13.93	11.69	9.31	9.62	12.88
s.d.		3.35	1.31	2.35	1.23	4.93
Min.		9.37	9.37	2.30	7.40	9.39
Max.		20.50	13.40	12.70	11.51	16.36
Haematite						
Mean	10.00	14.58	11.53	10.65	10.33	11.85
s.d.		4.67	1.09	2.50	1.70	1.04
Min.		9.45	9.45	6.80	7.80	11.11
Max.		22.80	12.90	16.70	14.00	12.58
Quartz						
Mean	5.16	7.01	6.57	5.90	6.30	6.37
s.d.		1.22	0.67	1.34	1.00	1.48
Min.		5.32	5.32	2.80	4.80	5.32
Max.		9.80	7.20	8.00	7.70	7.41
Gibbsite						
Mean	54.90	37.57	42.42	53.51	53.17	52.08
s.d.		6.59	3.32	4.84	3.35	13.26
Min.		28.30	40.13	40.00	47.81	42.70
Max.		49.78	49.78	64.60	59.00	61.45
Kaolinite						
Mean	3.02	3.94	4.25	4.60	4.21	1.52
s.d.		1.96	2.32	2.82	1.69	0.88
Min.		0.70	0.70	0.10	1.30	0.89
Max.		7.64	7.64	12.75	7.70	2.14
N		13	7	27	15	2

Figure 9
The type of preferred-orientation correction applied during the analysis of data (i) collected by participants and (ii) supplied by the CPD for sample 2. The number after each entry represents the number of analyses (including replicates) in each group.

reflects the spread in analyses of the crystalline phases. There is no significant difference within the participant-collected data results between physical inclusion of an internal standard and calculation based upon the supplied corundum figure. The inclusion of an appropriate empirical background shape into the methodology appears to be a successful strategy for assessment of amorphous content in both the CPD-supplied and participant-collected data. Such a shape has been obtained either by Le Bail fitting (Le Bail *et al.*, 1988) or by use of a physically based background as given by Riello *et al.* (1995). However, the population sizes for this method restrict an exhaustive evaluation.

3.3.4. Sample 4 – microabsorption problem. Tables 14 and 15 show the average AKLD values for all results returned for sample 4 partitioned according to microabsorption correction method employed for CPD-supplied and participant-collected data, respectively. Returns derived from participant-collected neutron data have been reported as a separate category of microabsorption 'correction' technique as neutron data should suffer little from microabsorption for these phases. Fig. 10 shows a summary of the types of microabsorption correction applied during the analysis of data for sample 4.

The high values of AKLD reported for all CPD-supplied data (Table 14) reflect the degree of severity of the microabsorption problem when data are collected using a coarse-grained sample. While there is a significant improvement in the results if the Brindley correction is applied, the AKLD values are still very high, suggesting that the extent of the microabsorption problem is really beyond the limits of the Brindley model in this case. Table 15 (participant-collected data) shows significantly lower AKLD values for all methods than those calculated for CPD-supplied data. This predominantly reflects the improvements due to size reduction during sample preparation. The majority of the 50th percentile group who had used X-ray data reported that they had ground the

width parameters at values typical of a highly crystalline phase.

Tables 12 and 13 show the average AKLD values for all results returned for sample 3 partitioned according to the amorphous-component calculation method employed for CPD-supplied and participant-collected data, respectively. These tables are derived from the data corrected for amorphous content by the authors. There is no significant difference in accuracy between the analyses performed on the CPD-supplied data and those of the participant-collected data. The only difference in methodologies is the opportunity for participants who collected their own data to incorporate a standard other than the corundum within the sample. By far the majority of participants opted for a calculation based upon the supplied corundum figure. The spread in the returns

sample prior to data collection. In most instances this fine-grinding was achieved through the use of the McCrone micronizing mill.

Within the participant-collected data group, the neutron returns are significantly better than the X-ray results regardless of whether microabsorption correction had been applied or not. However, the size of the neutron population restricts the drawing of statistically significant conclusions. The population sizes between the X-ray groups that employed either no microabsorption correction or the Brindley method are comparable (34 and 24, respectively). Between these groups it would appear that using the Brindley method is slightly better than the use of no correction at all but the deviations from the 'true' values remain high, again due to the fact that the extent of the microabsorption problem is probably beyond the range of the Brindley method.

Brindley classified non-homogeneous powders into four groups: fine, medium, coarse and very coarse (Brindley, 1945; Zevin & Kimmel, 1995), dependent upon μD where μ is the linear absorption coefficient of the phase and D is the particle diameter. For the mineral suite considered here, a particle size of 10 µm would result in the Brindley classification of the mixture as 'very coarse' for Cu $K\alpha$ and 'coarse' for Co $K\alpha$ X radiation. A classification of 'very coarse' renders the mixture unsuitable for the application of the Brindley model. The model can be applied to 'coarse' powders but the magnitude of the correction becomes very sensitive to the particle size chosen. As the Brindley model is particle-size dependent, any error in estimation of the particle size will be reflected in an error in the magnitude of the correction. In addition, the model assumes that the particles are spherical and of uniform size.

Table 8
Summary of the quantitative phase analyses derived from data (i) supplied by the CPD and (ii) collected by the participants for granodiorite.

Conventions and definitions are as per Table 4. Note that the 'All results' column refers to an average of the results from CPD-supplied and participant-collected data and the 'Authors' analyses'.

Phase	CPD-supplied data Participant returns	Participant-collected data X-ray Participant returns	Authors' analyses	Participant returns + authors' analyses	Neutron Participant returns	All results
Quartz						
Mean	30.46	31.70	29.20	30.85	31.19	30.64
s.d.	4.28	7.42	1.50	6.15	2.42	1.09
Min.	25.30	21.40	24.92	21.40	29.48	29.20
Max.	41.10	50.30	30.99	50.30	32.90	31.19
Feldspar						
Mean	15.44	15.51	19.66	16.94	14.88	16.37
s.d.	2.40	5.00	2.14	4.65	0.39	2.21
Min.	12.30	3.11	18.62	3.11	14.60	14.88
Max.	18.10	21.90	26.38	26.38	15.16	19.66
Albite						
Mean	41.34	38.76	40.35	39.31	40.05	40.13
s.d.	4.31	7.05	1.04	5.75	1.35	1.06
Min.	33.70	20.70	37.77	20.70	39.09	38.76
Max.	47.30	52.60	41.04	52.60	41.00	41.34
Biotite						
Mean	8.06	10.49	7.33	9.41	9.90	8.95
s.d.	2.83	4.32	0.61	3.81	0.56	1.49
Min.	3.48	2.10	6.48	2.10	9.51	7.33
Max.	11.10	23.70	8.71	23.70	10.30	10.49
Clinochlore						
Mean	2.39	1.60	2.30	1.84	2.15	2.11
s.d.	1.21	1.12	0.42	0.99	2.05	0.35
Min.	0.00	0.00	1.00	0.00	0.70	1.60
Max.	3.80	4.10	2.65	4.10	3.60	2.39
Hornblende						
Mean	2.06	1.91	1.14	1.65	1.62	1.68
s.d.	2.01	1.57	0.23	1.32	1.45	0.41
Min.	0.50	0.46	0.93	0.46	0.60	1.14
Max.	6.20	6.70	1.78	6.70	2.65	2.06
Zircon						
Mean	0.30	0.08	0.01	0.06	0.00	0.10
s.d.	0.42	0.20	0.02	0.18	0.00	0.14
Min..	0.00	0.00	0.00	0.00	0.00	0.00
Max.	1.20	0.90	0.06	0.90	0.00	0.30
N	10	23	12	35	2	47

Table 9
Summary of the quantitative phase analyses derived from data (i) supplied by the CPD and (ii) collected by the participants for pharmaceutical samples.

Results of individual analyses are shown as the numbers of returns are so low. Analysis #3 represents the average of three replicates from the same operator. All figures are wt%.

	Mannitol	Sucrose	Valine	Nizatidine	Starch
Pharmaceutical 1					
Weighed	45.0	35.0	10.0	10.0	
CPD-supplied data					
Analysis #1	58.6	12.1	5.0	24.3	
Participant-collected data					
Analysis #1	45.6	30.80	5.4	18.2	
Analysis #2	0.0	0.0	23.7	76.3	
Analysis #3	35.3	34.5	25.1	5.0	
Pharmaceutical 2					
Weighed	20.0	15.0	20.0	15.0	30.0
CPD-supplied data					
Analysis #1	58.6	12.1	5.0	24.3	0.0
Participant-collected data					
Analysis #1	55.5	12.0	8.4	24.1	0.0
Analysis #2	0.0	0.0	15.0	71.0	14.0
Analysis #3	19.4	19.9	20.4	7.4	32.9

Table 10
Average of the absolute values of the Kullback–Liebler distance for returned results for sample 2 partitioned according to preferred-orientation method employed – CPD-supplied data.

	Preferred orientation			
	None	March–Dollase	Spherical harmonics	Unknown
Average AKLD$_{sum}$	0.12 (12)	0.064 (23)	0.033 (1)	0.017 (–)
N	9	17	2	1

Table 11
Average of the absolute values of the Kullback–Liebler distance for returned results for sample 2 partitioned according to preferred orientation-method employed – participant-collected data.
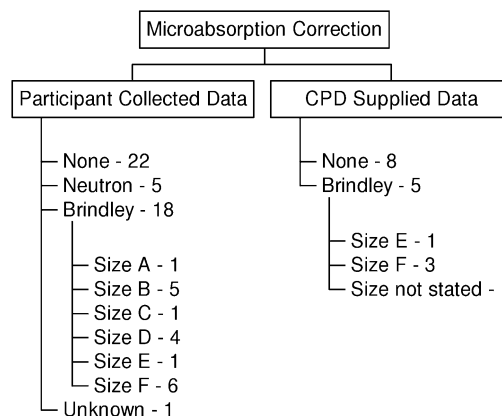
	Preferred orientation			
	None	March–Dollase	Spherical harmonics	Unknown
Average AKLD$_{sum}$	0.107 (54)	0.059 (13)	0.022 (8)	0.082 (32)
N	23	26	2	4

Table 12
Average of the absolute values of the Kullback–Liebler distance for returned results for sample 3 partitioned according to amorphous calculation method employed – CPD-supplied data.

	Amorphous calculation			
	Al_2O_3 as internal standard	Empirical background model	Crystalline quartz model	Unknown
Average AKLD$_{sum}$	0.11 (6)	0.069 (9)	1.3 (–)	0.3 (–)
N	15	2	1	1

Table 16 shows the average AKLD values for results obtained from X-ray diffraction studies performed by participant *A* and the authors for sample 4 partitioned according to microabsorption correction method and sample preparation employed. This study is independent of the bulk of the round-robin responses and examines directly the effects of grinding

Figure 10 diagram content:

Microabsorption Correction
- Participant Collected Data
  - None - 22
  - Neutron - 5
  - Brindley - 18
    - Size A - 1
    - Size B - 5
    - Size C - 1
    - Size D - 4
    - Size E - 1
    - Size F - 6
  - Unknown - 1
- CPD Supplied Data
  - None - 8
  - Brindley - 5
    - Size E - 1
    - Size F - 3
    - Size not stated - 1

For the Brindley correction model, the assumed particle sizes for the three phases reported by participants are :-

	Corundum μm	Magnetite μm	Zircon μm
Size A	3	3	3
Size B	5	5	5
Size C	8	8	8
Size D	12	12	12
Size E	8.4	36.2	21.1
Size F	28	36.2	21.1

Figure 10
The type of microabsorption correction applied during the analysis of data (i) collected by participants and (ii) supplied by the CPD for sample 4. The number after each entry represents the number of analyses (including replicates) in each group. The tabulated data are the assumed particle sizes in the Brindley correction model for the three phases reported by participants.

the sample. By far the worst results are obtained on the unground sample. Such a coarse specimen has grain-size problems (where non-representative peak intensities are observed) in addition to differences in μD. The Brindley correction model produces a slight improvement on the unground material, but the accuracy of the results is still poor (reflected in high AKLD values). This is caused by the presence of particle sizes and absorption contrasts that are well beyond the scope of the correction method. When the sample is ground there is only very slight improvement with use of the Brindley method over no correction at all. The level of uncertainty in the measurements produces slight overlap between these groups. This implies that the Brindley method is providing little additional improvement in microabsorption correction once the problem has been minimized through appropriate sample preparation.

The Brindley model for microabsorption correction appears to be bringing some improvement to quantitative phase analysis but is not nearly as effective as correction methods for other sample-related aberrations, such as preferred orientation (Tables 10 and 11). This suggests that while errors introduced by the presence of microabsorption are similar to those introduced by preferred orientation, the correction

Table 13
Average of the absolute values of the Kullback–Liebler distance for returned results for sample 3 partitioned according to amorphous calculation method employed – participant-collected data.

	Amorphous calculation					
	Al_2O_3 as internal standard	External standard	Internal standard	Empirical background model	Crystalline quartz model	Unknown
Average AKLD$_{sum}$	0.13 (4)	0.056 (–)	0.11 (5)	0.05 (–)	1.7 (–)	0.2 (2)
N	24	1	10	1	1	3

Table 14
Average of the absolute values of the Kullback–Liebler distance for returned results for sample 4 partitioned according to microabsorption correction methods employed – CPD-supplied data.

	Microabsorption correction	
	Brindley	None
Average AKLD$_{sum}$	0.33 (13)	0.63 (13)
N	5	8

Table 15
Average of the absolute values of the Kullback–Liebler distance for returned results for sample 4 partitioned according to microabsorption correction methods employed – participant-collected data.

Note that the neutron values have been reported as a separate category as they are largely unaffected by microabsorption.

	Microabsorption correction		
	Brindley	Neutron	None
Average AKLD$_{sum}$	0.11 (3)	0.031 (13)	0.20 (6)
N	24	5	34

Table 16
Average of the absolute values of the Kullback–Liebler distance for returned results for sample 4 partitioned according to microabsorption correction and whether additional sample preparation (i.e. grinding) was employed.

Results have been obtained from studies performed by participant A and the authors.

	Microabsorption correction/ sample preparation			
	Brindley		None	
	As received	Ground	As received	Ground
Average AKLD$_{sum}$	0.25 (12)	0.082 (18)	0.41 (5)	0.109 (10)
N	7	10	10	16

Table 17
Average of the absolute values of the Kullback–Liebler distance for returned results for synthetic bauxite partitioned according to preferred-orientation and microabsorption correction methods employed – CPD-supplied data.

	Preferred orientation/ microabsorption correction		
	Spherical harmonics	March–Dollase	
	None	Brindley	None
Average AKLD$_{sum}$	0.268 (30)	0.549 (22)	0.289 (65)
N	2	4	7

methods for microabsorption are less effective than those for preferred orientation.

3.3.5. Synthetic bauxite. Tables 17 and 18 show the average AKLD values for all returned results for synthetic bauxite partitioned according to preferred-orientation and microabsorption correction methods employed for CPD-supplied and participant-collected data, respectively. As stated previously (§3.3.1), there was a problem with the data set supplied by the CPD. It was therefore to be expected that participant-collected data would produce superior returns provided that appropriate sample preparation was carried out. This is demonstrated in the generally higher AKLD values for CPD-supplied data (Table 17) than those for participant-collected data (Table 18). However, within the CPD-supplied data there is a significantly higher AKLD value for those returns that have incorporated the Brindley method for microabsorption into their quantification strategy than for those with no correction. This suggests that the degree of correction made is inappropriate for the level of the problem in this sample. In sample 1 (Madsen *et al.*, 2001) the introduction of a sizeable microabsorption correction into a system in which very little was required produced increased errors in the results. It would appear that a similar effect is being observed here.

Table 18 shows a significantly higher AKLD value for one return, which included no preferred-orientation correction but which did employ the Brindley method for microabsorption correction. There is no significant difference between any of the other refinement strategies. Note, however, that the level of AKLD is high for all returns, indicating a poor ability to determine the phase abundances in this complex, but well defined, phase system.

3.3.6. Natural granodiorite. The accuracy of quantification of the phases present in the granodiorite remains ambiguous since the 'true' answer is not known as this is a naturally occurring material. This differs from the other samples in this round robin which are synthetic mixtures where the component phases are all known and have been weighed out in known proportions. The phase identification supplied with the granodiorite was a basic description and not meant to restrict participants from including greater detail (i.e. more than one feldspar structure) in their quantification. The mean values returned by participants are given in Table 8 along with determinations by the authors. The authors' values are based on 12 analyses conducted by two different operators on behalf of the authors on 12 micronized sub-samples of the granodiorite as issued to the participants. Six of the 3 g samples were micronized for 24 min, while the other six were micronized for 48 min. Data were collected under the same conditions as all other CPD-supplied data and analysed using the *Koalariet* (Coelho *et al.*, 1997) software for Rietveld analysis. 'Participant returns + authors' analyses' includes the authors' analyses with the other X-ray returns. The 'Total' column refers to an average of the results from CPD-supplied and participant-collected data and the 'Authors' analyses'.

Table 18
Average of the absolute values of the Kullback–Liebler distance for returned results for synthetic bauxite partitioned according to preferred-orientation and microabsorption correction methods employed – participant-collected data.

	Preferred orientation/microabsorption correction						
	Spherical harmonics	None		Unknown		March–Dollase	
	Brindley	Brindley	None	None	Unknown	Brindley	None
Average AKLD$_{sum}$	0.154 (–)	0.295 (–)	0.164 (71)	0.202 (94)	0.140 (32)	0.106 (36)	0.155 (46)
N	1	1	7	3	3	5	11

Table 19
Average of the absolute values of the Kullback–Liebler distance for all returned results partitioned according to the type of radiation used to collect data.

	CPD-supplied X-ray	Neutron	Synchrotron	Participant-collected laboratory X-ray
Sample 2				
Average AKLD$_{sum}$	0.102 (48)	0.028 (11)	0.042 (25)	0.088 (27)
N	29	6	2	47
Sample 3				
Average AKLD$_{sum}$	0.99 (73)	2.6 (2.6)	0.11 (–)	0.50 (37)
Average ALKD$_{sum}$ (corrected for amorphous content by authors)	0.18 (13)	0.045 (35)	0.11 (–)	0.182 (95)
N	19	3	1	36
Sample 4				
Average AKLD$_{sum}$	0.50 (14)	0.071 (82)	0.15 (–)	0.193 (57)
N	13	6	1	39
Synthetic bauxite				
Average AKLD$_{sum}$	0.366 (79)	–	0.24 (10)	0.150 (27)
N	13	–	2	26
All samples				
Average AKLD$_{sum}$	0.490 (87)	0.90 (71)	0.135 (71)	0.233 (30)
Average ALKD$_{sum}$ (corrected for amorphous content by authors)	0.287 (42)	0.048 (11)	0.135 (74)	0.153 (8)
N	74	17	5	148

The relatively low standard deviations in the 'Total' column suggest a reasonable degree of agreement across the participant means. This provides the best estimate of the phase abundances in the granodiorite sample.

3.3.7. Pharmaceutical samples. There seems to have been a general reluctance of the community to even attempt analysis of the pharmaceutical samples. There were very few requests for samples in the initial expressions of interest in the round robin and only three participants returned any type of analyses. In subsequent investigation by the authors, it has been discovered that the samples were probably beyond the scope of a round robin dealing solely with QPA. The predominant reason for this is the incomplete structural information supplied by the CPD for at least one of the crystalline phases included in the mixtures. This was compounded by the crystal habits of two of the component phases: one being very thin flat plates and the other being needles. This lead to severe preferred orientation which further complicated the analytical procedure.

It is unfortunate that these samples were not an ideal test for quantitative phase analysis of pharmaceutical materials. However, it is also unfortunate that the community as a whole appears to regard the pharmaceutical industry as being outside its area of expertise. This is an area that requires further investigation, as QPA information may prove beneficial to this constantly expanding industry.

3.3.8. Overview of instrument type. Table 19 shows an average of the absolute values of the Kullback–Liebler distance for samples 2, 3, 4 and synthetic bauxite results partitioned according to the type of radiation used to collect data. If all samples are considered together on the basis of the as-received results, the participant-collected X-ray and synchrotron data results are of similar accuracy and are significantly better than those from the CPD-supplied data and participant-collected neutron data. This situation changes somewhat if the correction for amorphous content in sample 3 is performed where the participants have omitted it. Then, the participant-collected neutron returns are significantly better than any of the others, while there is no significant difference between those from participant-collected synchrotron and X-ray data. This is a fairer assessment of data collection methods as the failure to calculate the amorphous content is an easily remedied operator error. The returns from CPD-supplied data are still significantly worse than those from participant-collected data. This is due to the fact that most of the data provided by the CPD was collected on the as-supplied samples. Thus, it is to be expected that participant-collected data would outperform CPD-supplied where appropriate additional sample preparation was performed.

Table 19 also shows the breakdown of results within each sample group. For sample 2, the returns from participant-collected neutron data are significantly better than any of the others. However, due to the fact that there are only six analyses in the neutron group, this may be more related to operator expertise than a true difference resulting from the data collection method. The largest groups of analyses are on CPD-supplied X-ray data and participant-collected X-ray data. While there are large differences between the AKLD values, the spread of values within each group (reflected in the

large uncertainties) renders these differences statistically insignificant.

If the as-received results for sample 3 are considered, there is a wide spread in the neutron analyses, largely due to the fact that in two of the three analyses the amorphous component has not been calculated. However, when the amorphous content is calculated, the results more accurately represent the weighed values. As with sample 2, there is no significant difference between the CPD-supplied and participant-collected X-ray groups.

For sample 4 the returned analyses of CPD-supplied data are significantly worse than any participant-collected data. This is due to the fact that the CPD-supplied data were collected on a coarse grained specimen which enhances the severe microabsorption problem. Participant-collected X-ray data have achieved improved results predominantly through additional sample preparation conducted by participants (presumably fine grinding, but incomplete details were returned to the CPD). It would be expected that the effects of microabsorption on neutron data would be minimal. However, the spread of neutron returns was such that the difference between the neutron and participant-collected X-ray data is at the limit of significance. Once again the population size of the neutron group prohibits the drawing of any further conclusions in this regard.

As previously discussed (§3.3.1), the CPD-supplied X-ray data for the synthetic bauxite were collected on the sample as supplied to the participants. The participant-collected data results are significantly better than those achievable from the CPD-supplied data, predominantly through sample preparation, *i.e.* grinding to release the individual particles of all phases. Subsequent analysis of micronized synthetic bauxite by the authors has provided more accurate estimates of the 'true' values than those obtainable from the CPD-supplied data.

3.3.9. Overview of analysis type. Table 20 shows an average of the absolute values of the Kullback–Liebler distance for returned results on CPD-supplied data partitioned according to the analytical method employed. In this instance the majority of returns (71) used Rietveld-based methods with only a few (three) using RIR methods. As a consequence of this, little can be made of the efficacy of one method over the other. Table 21 shows similar results for participant-collected data, where a wider range of analytical methods was used. The majority of the analyses still used the Rietveld method (137), with the next most commonly used method (23) being RIR. A few other returns were provided using full-pattern analysis (six), iterative least squares (three) and internal-standard (one) methods. Once again data have been quoted with and without the authors' correction for amorphous content in sample 3. This only affects the Rietveld figures as the only analyses in which this correction had been omitted were made using the Rietveld method.

In both Tables 20 and 21 the data have also been broken down into a summary of each sample's returns. On a sample by sample basis, the small populations of methods other than that of Rietveld restricts the drawing of statistically meaningful

Table 20
Average of the absolute values of the Kullback–Liebler distance for returned results partitioned according to analytical method employed – CPD-supplied data.

	Rietveld	RIR
Sample 2		
Average $AKLD_{sum}$	0.101 (49)	0.149 (–)
N	28	1
Sample 3		
Average $AKLD_{sum}$	1.04 (77)	0.280 (–)
Average $ALKD_{sum}$ (corrected for amorphous content by authors)	0.17 (14)	0.280 (–)
N	18	1
Sample 4		
Average $AKLD_{sum}$	0.47 (15)	0.465 (–)
N	12	1
Synthetic bauxite		
Average $AKLD_{sum}$	0.366 (79)	–
N	13	0
All samples		
Average $AKLD_{sum}$	0.494 (94)	0.30 (18)
Average $ALKD_{sum}$ (corrected for amorphous content by authors)	0.277 (41)	0.30 (18)
N	71	3

conclusions regarding the performance of individual methods, but indicates a clear preference for Rietveld-based methods by the diffraction community. If all analyses are considered as-received, the Rietveld method appears to have performed slightly worse than the other methods. If the authors' correction for amorphous content in sample 3 is included, there is no significant difference in the results from different analytical methods. However, where the populations are very small, this may be more a reflection of operator expertise than efficacy of the method in general.

4. Discussion

By far the greatest numbers of returns of both CPD-supplied and participant-collected data were derived from Rietveld-based methods. Consequently the bulk of the subsequent data analysis has been concerned with this method. There are a number of analytical issues that represent the main areas of concern threatening the success of QPA *via* diffraction methods. They do not cover all sources of error noted in the returns but are the dominant problems which must be addressed first.

4.1. Microabsorption correction

The problem of microabsorption appears to be the biggest physical hindrance to accurate quantitative phase analysis using X-ray diffraction data. The problem is virtually absent in neutron diffraction data; this is confirmed with the neutron participants achieving much more accurate results with sample 4. However, this cannot be accepted as definitive because of the relatively low population size of the neutron returns. The

Table 21
Average of the absolute values of the Kullback–Liebler distance for returned results partitioned according to analytical method employed – participant-collected data.

	ILS	Rietveld	Full-pattern analysis	RIR	Internal standard
Sample 2					
Average $AKLD_{sum}$	0.152 (–)	0.055 (10)	0.069 (3)	0.20 (12)	0.129 (–)
N	1	43	2	8	1
Sample 3					
Average $AKLD_{sum}$	0.122 (–)	0.77 (50)	–	0.16 (10)	–
Average $ALKD_{sum}$ (corrected for amorphous content by authors)	0.122 (–)	0.17 (10)	–	0.16 (10)	–
N	1	32	0	7	0
Sample 4					
Average $AKLD_{sum}$	0.093 (–)	0.182 (53)	0.090 (9)	0.18 (13)	–
N	1	38	2	5	0
Synthetic bauxite					
Average $AKLD_{sum}$	–	0.152 (29)	0.257 (86)	0.127 (70)	–
N	0	24	2	3	0
All samples					
Average $AKLD_{sum}$	0.122 (34)	0.289 (56)	0.139 (84)	0.167 (65)	0.129 (–)
Average $ALKD_{sum}$ (corrected for amorphous content by authors)	0.122 (34)	0.140 (24)	0.139 (84)	0.167 (65)	0.129 (–)
N	3	137	6	23	1

X-ray participants who had the most success with sample 4 were those who had taken some care with sample preparation. This mainly involved the reduction in particle size of the sample by grinding to minimize the microabsorption problem.

The most commonly used correction method for micro-absorption was that of Brindley (1945) in conjunction with Rietveld pattern analysis methods. A slight improvement in results was achieved when the Brindley method was applied, but it would appear that, in this instance, the severity of the problem was beyond the limits of the correction algorithm. The Brindley method was most successful when combined with sample preparation strategies that minimized the problem prior to data collection. This result was supported by the separate study undertaken by the authors and participant A examining the effects of grinding the sample prior to data collection.

The effects of the application of a microabsorption correction strategy to a sample in which microabsorption is not a major problem became apparent in the analysis of returns from sample 1 in this round robin (Madsen *et al.*, 2001). The degree of overcorrection produces considerable inaccuracy in the final reported quantification. This finding has been supported here in the analysis of the synthetic bauxite sample. In most instances where a microabsorption correction (Brindley) had been applied, the results were less accurate than where the correction was not applied. Table 1 shows the mass absorption coefficients for all the phases within the synthetic bauxite sample. For Co $K\alpha$, the wavelength most commonly used by the participants with AKLD values in the top 50th percentile, there is little absorption contrast between the major phases. With Co $K\alpha$, anatase has a high absorption coefficient but it is only present at the 2 wt% level. It would

appear that in this sample the presence of fine particle sizes has resulted in a minimal microabsorption problem. In this instance, the application of a correction model like that of Brindley has served to reduce the accuracy of the quantitative phase analysis rather than bring any improvement.

4.2. Operator error during analysis

The problem of operator error for these samples is as great as it was for sample 1 (Madsen *et al.*, 2001). Operator error can begin in the sample preparation stage and extend throughout subsequent data collection and analysis. One of the most basic sources of error was the failure of some participants to grind samples, even when they were clearly too coarse for successful data collection and analysis.

There is also continued demonstration of a lack of crystal-lographic and chemical understanding, particularly with respect to the use of Rietveld refinement techniques. This is evidenced by the following specific examples exhibited by a number of participants who supplied their output files with their returns: (i) the acceptance of very high values of the various measures of fit, such as the weighted profile R factor and Bragg R factors, without examination of the refined parameters and continuing the refinement to completion; (ii) acceptance of physically unrealistic parameters, *i.e.* thermal parameters with magnitudes of the order of 10 Å^2; (iii) the refinement of parameters that the data cannot support (*i.e.* refinement of structural parameters of phases present at only a few wt%); (iv) the failure to correct for amorphous content in sample 3 despite its obvious presence in the pattern; (v) the use of an inappropriate model for amorphous component (*i.e.*

Table 22
Minimum and maximum values of errors reported for samples 2, 3 and 4.

Phase	Weighed amount (wt%)	Reported error estimates			
		CPD-supplied data		Participant-collected data	
		Minimum	Maximum	Minimum	Maximum
Sample 2					
Corundum	21.27	0.1	19.9	0.0	25.9
Fluorite	22.53	0.1	10.2	0.0	4.0
Zincite	19.94	0.0	5.3	0.0	3.0
Brucite	36.26	0.0	3.0	0.0	7.0
Sample 3					
Corundum	30.79	0.0	6.9	0.0	7.8
Fluorite	20.06	0.0	5.2	0.0	5.9
Zincite	19.68	0.0	8.0	0.0	5.0
Amorphous	29.47	0.0	3.0	0.0	13.6
Sample 4					
Corundum	50.46	0.0	4.9	0.0	20.5
Magnetite	19.64	0.0	19.1	0.0	29.1
Zircon	29.90	0.0	5.3	0.0	9.8

including highly crystalline quartz in the refinement strategy as a model for amorphous silica).

While these examples demonstrate common problems, the numbers of participants who returned this level of detail precluded the statistical analysis of such errors.

4.3. Error estimation

Table 22 shows the spread of error estimates reported by users over samples 2, 3 and 4. Many users returned no estimation of error with their results. Methods of error calculation were generally not reported but some values returned appeared to be the errors calculated by Rietveld-based software. The derivation of absolute errors in such a standardless method as that of Rietveld is no simple matter. However, it is inappropriate to quote errors based solely on the mathematical precision of the fit of the model to the observed data as such since they are underestimated in relation to the 'true' errors in the analysis. In contrast, the magnitude of some of the errors reported was extremely high and may have been intended to represent relative percentage errors. However, this was not specified anywhere in the participant returns.

It is beyond the scope of this round robin to carry out a detailed study of the calculation of errors on QPA. Participants were not requested to supply details of their methodology so no conclusions can be drawn regarding this. The calculation of meaningful errors is an extremely important part of quantitative phase analysis and as such must be considered in future studies. The returns indicate that there is currently little standardization in approach to calculating these errors.

5. Conclusions

The samples reported in this paper reinforce the findings based upon sample 1 and reported by Madsen *et al.* (2001). The major obstacles to QPA *via* diffraction methods are (i) the physical problem of microabsorption for X-ray diffraction and (ii) the problems of operator error or lack of knowledge in sample preparation and analysis.

The problem of microabsorption with X-rays is so severe that it just may not be possible to examine some suites of materials successfully using the current methodology. However, in many cases the problem may be minimized through appropriate sample preparation techniques, selection of wavelength to avoid strong absorption contrast and in some instances the application of mathematical correction models such as that of Brindley (1945). There is a risk associated with the use of such models, clearly demonstrated in the results for sample 1 in the previous study and the synthetic bauxite in the current work. That risk is the one of overcorrection, particularly where a correction is applied when, in fact, none is required. It is therefore of primary importance for operators to establish whether or not such a correction is necessary and only then to apply it. Empirical correction models could be derived, but these would be specific to the phase suites and particle sizes for which they were derived.

The problems relating to operator expertise may be addressed by the provision of regular workshops in sample preparation and analytical techniques and the use of training publications, such as that of McCusker *et al.* (1999). Such education is the responsibility of the diffraction community as a whole and is as important to its advancement as the continued developments in mathematical modelling and instrument design.

6. Recommendations

6.1. Rietveld refinement

The predominance of Rietveld-based methods for QPA makes it of vital importance for the community to establish some standardization in pattern analysis methodology. This may be achieved through education programmes for users but should also entail the development and provision of a list of Rietveld refinement strategies that includes a checklist of

acceptable parameter values. While such a list may also be able to be encoded into the various software packages, it is dangerous to attempt to reduce complex scientific processes such as Rietveld refinement into 'black box' technology. Even with more 'intelligent' software, there must be general improvement in operator expertise. The provision of a certain 'minimum' level of crystallographic information to non-crystallographers is essential as the use of Rietveld-based methods continues to expand.

6.2. Sample preparation and data collection

It is of the utmost importance that sample preparation and data collection methodology be appropriate for the task at hand. It should become a routine part of diffraction analysis to establish the requirements for sample preparation based upon the inherent problems of the particular sample. It may be necessary for X-ray users to calculate the mass absorption coefficients for the component phases to determine whether or not microabsorption may be an issue. If it is, the particle size of the sample may need to be measured and reduced accordingly. Such knowledge will also allow the selection of the most appropriate wavelength for the task.

Where a sample exhibits preferred orientation it may be possible to minimize the effect in the data by judicious choice of sample presentation mode (*i.e.* back pressing or capillary sample). This is essential for users of non-Rietveld-based methods and it may also be advisable for Rietveld users, even though mathematical correction models, such as the March–Dollase and spherical harmonics models, appear to work quite well. It should be remembered, however, that all of these correction models are only approximations and that any sample-related problems should be minimized prior to data collection.

The nature of the data needed to fulfil the analysis requirements also needs to be carefully considered. The choice of instrument type (laboratory X-ray, neutron, synchrotron), wavelength, sample presentation (flat plate, capillary), range of diffraction angle collected (2θ), increment size in 2θ and step counting time are all parameters which may have an impact on the final result. However, local folklore or time pressures often dictate data collection protocol, rather than an approach that considers sample and analytical issues. A more detailed discussion of these issues has been presented by Hill & Madsen (2002).

6.3. Error estimation

The range of errors reported in this study (Table 22) reflect the lack of standardization of any method for their calculation. This is the same situation as reported for sample 1 (Madsen *et al.*, 2001). This further study only reinforces that finding and emphasizes the need for the development of the methodology required to provide meaningful estimates of error in QPA.

6.4. Education

The subject of education has been touched on in specific reference to the Rietveld method, but it is the belief of the authors that the community as a whole must address education with regards to quantification of phase mixtures from a wider perspective. It is necessary that people not only become familiar with the basics of crystallography but with the even more basic fundamentals of sample handling and preparation, data collection strategies, phase identification, choice of quantification method appropriate to the task, choice of parameters within that method and assessment of results. In short, it is recommended that a practitioners guide be developed and used as a basic educational tool in forums such as those provided by the IUCr, various national committees for crystallography, the IXAS, the ICDD and other such organizations.

6.5. Further work

This round robin was devised to test broadly the methods used by powder diffractionists when obtaining quantitative phase abundances from multiphase mixtures. Accordingly, the methods to be used were not specified by the organizers and were left to the discretion of individual participants. As such, the round robin acted as a survey of instrumentation and analytical methods commonly used in QPA. The authors therefore recommend that an additional study be undertaken (with a smaller number of samples) in which detailed methods of sample preparation, data collection and analysis are specified to the participants. This should serve to minimize the spread of results observed in the current study, which could often be attributed to poor analytical practice. The new study might focus on an industrially important phase system such as the measurement of respirable silica in multiphase mixtures. In this way, standard methods and practices may be determined for common analytical problems.

References

Brindley, G. W. (1945). *Philo. Mag.* **7**, 36, 347.

Coelho, A. A., Madsen, I. C. & Cheary, R. W. (1997). *A New Rietveld Refinement Program Using a Fundamental Parameters Approach to Synthesizing Line Profiles*, Abstract D1-PM2, *Proceedings of the 20th Conference of the Society of Crystallographers in Australia*, 2–5 April, Queenstown, New Zealand.

Dollase, W. A. (1986). *J. Appl. Cryst.* **19**, 267–272.

Hill, R. J. (1992). *J. Appl. Cryst.* **25**, 589–610.

Hill, R. J. & Cranswick L. M. D. (1994). *J. Appl. Cryst.* **27**, 802–844.

Hill, R. J. & Howard, C. J. (1986). *A Computer Program for Rietveld Analysis of Fixed Wavelength X-ray and Neutron Powder Diffraction Patterns*. AAEC (now ANSTO) report AAEC/M112.

Hill, R. J. & Madsen, I. C. (2002). *Sample Preparation, Instrument Selection and Data Collection*, in *Structure Determination from Powder Data*, edited by W. I. F. David, K. Shankland, L. B. McCusker & Ch. Baerlocher, ch. 6. Oxford University Press.

Hill, R. J., Tsambourakis, G. & Madsen, I. C. (1993). *J. Petrol.* **34**, 867–900.

Knudsen, T. (1981). *X-ray Spectrom.* **10**, 54–56.

Kullback, S. (1968). *Information Theory and Statistics*, pp. 1–11. New York: Dover.

Le Bail, A., Duroy, H. & Fourquet, J. L. (1988). *Mater. Res. Bull.* **23**, 447–452.

Leventouri, T. (1997). *Physica C*, **277**, 82–86.

McCusker, L. B., Von Dreele, R. B., Cox, D. E., Louer, D. & Scardi, P. (1999). *J. Appl. Cryst.* **32**, 36–50.

Madsen, I. C., Scarlett, N. V. Y., Cranswick, L. M. D. & Lwin, T. (2001). *J. Appl. Cryst.* **34**, 409–426.

Rafaja, D. & Valvoda, V. (1996). *Round Robin on Quantitative Phase Analysis*. Praha: Krystalografická společnost.

Riello, P., Fagherazzi, G., Clemente, D. & Canton, P. (1995). *J. Appl. Cryst.* **28**, 115–120.

Rietveld, H. M. (1969). *J. Appl. Cryst.* **2**, 65–71.

Von Dreele, R. B. (1997). *J. Appl. Cryst.* **30**, 517–525.

Zevin, L. S. & Kimmel, G. (1995). *Quantitative X-ray Diffractometry*, edited by I. Mureinik. New York: Springer-Verlag.